

## SYNTHESIS OF NANOCOMPOSITES WITH PARTICIPATION OF BSCCO SUPERCONDUCTING PHASES, RGO AND AgNPs

Janna Mateeva, Anna Staneva

University of Chemical Technology and Metallurgy  
8 Kliment Ohridski blvd., 1756 Sofia, Bulgaria  
E-mail: ani\_sta@uctm.edu

Received 13 May 2023  
Accepted 05 June 2023

---

### ABSTRACT

Reduced graphene oxide (RGO) and silver nanoparticles (AgNPs) have been used to prepare (Bi-2223) composites. The structural and morphological properties of the synthesized initial components and the composites are characterized using X-ray diffraction and Transmission electron microscopy. Two high-temperature superconducting orthorhombic phases of Bi-2223 and 2212 are synthesized at a temperature of 830°C for 16 hours in air. TEM images of the composite confirm the presence of silver nanoparticles (Ag-cubic) with an approximate size of about 10 nm and the specific structure of reduced graphene oxide sheets. Significant exfoliation of the graphene oxide and successful reduction leading to the observation of smooth and singular RGO layers.

Keywords: BSCCO superconducting ceramics, RGO, Ag NPs, TEM, structure, nanocomposites.

---

### INTRODUCTION

The study of superconductivity is one of the main problems that mark the development of modern science - physics, chemistry, material science. The main branches of research from the modern materials science perspective are: synthesizing new ceramic superconducting materials with a high critical temperature of the superconducting transition; development of new synthesis technologies; obtaining structures with a certain orientation of the microcrystals; increasing the density of ceramics; increasing the mechanical strength and chemical resistance; replacing expensive raw materials with cheaper and more accessible ones; studying the influence of various additives to improve physical and chemical properties; development of new tape and wire drawing technologies; obtaining details with a complex profile, layers, single crystals and so on. The main unsolved challenges to the widespread use of ceramic superconductors are the still low critical temperature values, the critical current density and the critical magnetic field, the unsatisfactory mechanical strength, the difficulties in making strips, threads and layers (due to the fragility of the material), as well as the low chemical resistance.

Among the known high temperature superconductors, the most commonly studied compound is BSCCO because it is being the first high temperature superconductor discovered which does not contain rare-earth elements and it has a high critical temperature [1]. BSCCO is a cuprate high-temperature superconductor, sharing a two-dimensional layered perovskite structure with superconductivity taking place in a copper-oxide plane. The  $\text{Bi}_2\text{Sr}_2\text{Ca}_2\text{Cu}_3\text{O}_{8+x}$  phase (known as 2223 phase) exhibits the highest critical temperature among all the BSCCO phases. It is a high temperature superconductor with many applications including magnets [2 - 4], HTS wires [5], electrical power devices [6, 7] among others.

A lot of work has been done in recent years to study the influence of various additives to superconducting materials to improve their physical and technological parameters. Repeated attempts have been made to dope superconducting ceramics with  $\text{Ag}_2\text{O}$  in order to improve the superconducting properties of the material [8 - 10]. Silver is an impurity that diffuses very quickly in superconducting materials. Significant diffusion penetration of Ag into the material is observed even at room temperature. The high mobility of silver atoms and the possibility of interaction of Ag with the components of the superconductor can lead to structural changes

during the heat treatment. The resulting materials contain several phases and most of the silver is located between individual grains of the superconducting phases. An important advantage of the silver as an additive to the superconductor is that it helps the diffusion of the oxygen into the bulk material during synthesis. When small amounts of silver are added, an increase of critical temperature ( $T_c$ ) of the superconducting sample is observed. Silver has a high coefficient of thermal conductivity so it is often used as an additive to superconductors, and the thermal conductivity of the composites with added silver has been found to increase. One of the earliest and promising studies on the introduction of silver into BSCCO superconductor was proposed by M. Muralidhar et al. [11]. Subsequently, the team has investigated the electrical and magnetic properties of a BPSCCO phase doped with Ag with a nominal composition of  $\text{Bi}_{1.7}\text{Pb}_{0.3}\text{Ag}_x\text{Sr}_2\text{Ca}_2\text{Cu}_3\text{O}$  ( $x=0-3$ ). It has been shown that the superconducting properties do not deteriorate with the addition of silver. The transition to the superconducting state is sharper and the critical current density  $J_c$  increases with the increasing of silver content. It is assumed that Ag is distributed at the grain boundary and thus improves the bonds between the grains. Silver also enhances the mechanical properties of the high-temperature superconductors, which is essential for their practical application [12].

A complex study on the influence of Ag on the superconductivity of BSCCO was done in 2010 [13]. A ceramic with a nominal composition of BSCCO - 2212 was synthesized by a solid-state reaction at 820°C for 20 hours in corundum crucibles. The resulting materials were ground again and mixed with the additions of MgO,  $\text{AgNO}_3$  and  $\text{Pr}_6\text{O}_{11}$ . The samples without additives have a critical temperature  $T_c$  of 65 K, while the Mg- and Ag-containing phases have  $T_c$  of 77 K and 75 K, respectively. Pr-containing samples are not superconducting. Great successes have been achieved in the industry for the production of BSCCO - 2223/Ag high-temperature superconducting tapes [14]. The way of connecting the individual particles in an Ag tube is still an unsolved problem, since it significantly affects the electrical and superconducting properties. The  $J_c$  property of BSCCO - 2223/Ag tape in the presence of external magnetic field compared to YBCO superconductor, is still poor. One of the ways to increase the critical current density is doping the superconducting phases with nanostructured

materials [15], thereby reducing weak connections and creating pinning centers.

Combining superconductors with graphene in composite materials would result in superconducting properties at temperatures below the critical temperature and good electrical conductivity at higher temperatures of the composite. Graphene is a promising material in many applications because of its outstanding properties, such as ultrahigh carrier mobility, excellent electrical conductivity, high thermal conductivity, large theoretical specific surface area, high optical transmittance, high Young's modulus, and outstanding mechanical flexibility. Therefore, a large number of sensors with high sensitivity, selectivity and stability have been created in recent years using graphene materials. Combining graphene with various functional nanomaterials (precious metals, metal compounds, carbon materials, polymer materials, etc.) results in unique optical, mechanical, electrical, chemical and catalytic properties. The controlled production of nanoparticles drives nanotechnology and makes it one of the most promising and popular fields of scientific research today.

Graphene is considered an excellent thermal conductor and several studies have investigated its unlimited potential for thermal conductivity based on sample size [16]. In both computer simulations and experiments, the researchers found that the larger the graphene segment is, the more heat it can carry. Theoretically, graphene can conduct an unlimited amount of heat. Thermal conductivity increases logarithmically as the area of the carbon monolayer enlarges, and the researchers believe this may be due to the stable bonding pattern of the carbon atoms, as well as the fact that it is a two-dimensional (2D) material. Since graphene is significantly more tear-resistant than steel and it is also light and flexible, its conductivity could have some attractive real-world applications.

The values of the coefficient of thermal conductivity vary within wide limits and depend on the method of preparation, as well as on the number of carbon layers. The highest values measured for exfoliated single-layer graphene (SLG) are 3000 - 5000 W/m K [17]. It has been shown that the addition of graphene flakes in various composites and nanostructured materials can dramatically increase the thermal conductivity of the resulting composite materials [18, 19]. It is interesting to investigate the thermal properties of such graphene

composites, and in particular the dependence of the thermal conductivity on the concentration of graphene in the composites [20].

There are limited numbers of studies on the synthesis and characterization of superconducting YBCO ceramics with the addition of different graphene structures - graphene, graphene oxide or reduced graphene oxide [21 - 28]. The main direction in the experiments is focused on studying the influence of graphene on the critical temperature of the superconducting composite. An increase in the critical temperature of the superconductor when adding GO and RGO in different ratios has been reported. It is noteworthy that the influence of graphene materials on the thermal conductivity of superconducting ceramics has not been investigated so far.

The influence of silver nanoparticles and carbon nanotubes (CNTs) on the mechanical properties of YBCO superconducting samples has also been investigated. It is observed from the results that the crystallite size, the lattice strain, and the strain of the YBCO samples decrease when CNTs and Ag nanoparticles are added to the compounds. The influence of CNTs on the properties of the composite is more effective than the influence of Ag nanoparticles [29].

Graphene materials possess extremely good thermal properties and their addition to superconducting ceramics would lead to an increase in the thermal conductivity of the resulting composites. Silver improves the mechanical properties and physical characteristics of ceramic superconductors. There is no literature data on research and obtaining composites with the participation of BSCCO phases, silver nanoparticles and graphene structures.

The aim of the present study is to synthesize and structurally characterize nanocomposites with the participation of BSCCO superconducting phases, silver nanoparticles and reduced graphene oxide. In the future, it is planned to determine the physical and thermal properties of the obtained composites.

## EXPERIMENTAL

### Materials and methods

The starting components BSCCO, RGO and AgNPs and the composites BSCCO/AgNPs and BSCCO/RGO/AgNPs were synthesized and the structurally characterized using XRD, TEM and HRTEM.

For the synthesis of BSCCO phase we used the initial

oxides and carbonates:  $\text{Bi}_2\text{O}_3$ ,  $\text{SrCO}_3$ ,  $\text{CaCO}_3$ ,  $\text{CuO}$ . All raw material quantities were converted from moles to mass percentages. The initial materials in the required stoichiometric ratios were mixed and homogenized in an agate mortar for one hour, then the powder was tableted with a pressure of 5 - 6 MPa and fired at a temperature of 830°C for 16 hours in air.

The reduced graphene oxide was obtained by chemical exfoliation of purified natural graphite powder by Hammer's method and subsequent reduction with sodium borohydride. The first step is the oxidation of graphite to obtain graphite oxide. Flake graphite was ground then concentrated sulfuric acid, phosphoric acid, and sodium nitrate were gradually added to the graphite powder in an ice bath with constant stirring. Potassium permanganate was added to the mixture and stirring continued for another hour in the ice bath. Then distilled water was added dropwise (under a fume hood) for 1 hour. Every process was done at room temperature. The mixture was allowed to sit for 24 hours then we slowly added drop by drop a solution of distilled water and 30 % hydrogen peroxide, with constant stirring at room temperature. The second step is the exfoliation of the individual graphene layers and their reduction. The resulting solution was sonicated in an ultrasonic bath for two hours. Sodium hydroxide (NaOH) was used to alkalinize the solution. Sodium borohydride ( $\text{NaBH}_4$ ) was added as a reducing agent. After stirring for 1 hour the solution was left to sit for 24 hours at room temperature.

Ag NPs were obtained from silver nitrate by a green reduction method using L-ascorbic acid. The two solutions - 0.2 M solution of silver nitrate ( $\text{AgNO}_3$ ) and 0.1 M L-ascorbic acid ( $\text{C}_6\text{H}_8\text{O}_6$ ) were made separately and heated to 60°C under constant stirring with a magnetic stirrer. The silver nitrate solution is added dropwise to the ascorbic acid solution at active stirring with a magnetic stirrer. After stirring at 60°C for one hour, the mixture was allowed to cool to room temperature and the resulting precipitate was filtered off under vacuum. It was washed three times with distilled water and dried in a laboratory vacuum dryer at 60°C. Gray-white fine powder was obtained.

BSCCO composites series was obtained with addition of 5 or 10 mass % AgNPs to BSCCO phase. All the samples were mixed, homogenized in an agate mortar and tableted (Table 1).

Table 1. BSCCO composites series designation and composition.

Designations	Composition
B	BSCCO
B5	BSCCO + 5 mass % AgNPs
B10	BSCCO + 10 mass % AgNPs
10B5	BSCCO + 5 mass % AgNPs +10 mass % RGO

Table 2. Phases determined by SAED analysis of BSCCO.

No	Phase	COD/PDF	Lattice parameters, [Å]	S.G.
I	$\text{Bi}_2\text{Sr}_2\text{CaCu}_2\text{O}_8$ Orthorhombic	#96-100-0286	a = 5.4054 b = 5.4016 c = 30.7152	Amaa
II	$\text{Bi}_2\text{Sr}_2\text{Ca}_2\text{Cu}_3\text{O}_x$ Orthorhombic	45-1223	a = 5.42 b = 5.44 c = 36.76	

## RESULTS AND DISCUSSION

### Superconducting phases in Bi-Sr-Ca-Cu-O system

The XRD patterns of the obtained samples are presented in Fig. 1. For this purpose, a Bruker D8 Advance apparatus with Cu  $K\alpha$  radiation was used. It can be seen that the two high temperature superconducting phases 2212 (compared with reference X-ray card JSPDS 00-045-0676 of phase 2212) and 2223 (JCPDS 00-043-0088) were obtained as a result of the solid phase synthesis. The basis for this assumption is the presence of intense peaks around the 27, 33 and 35  $2\theta$  degree.

Transmission Electron Microscope JEOL JEM 2100 was used for bright field (BF) TEM, high resolution (HR) TEM and selected area electron diffraction (SAED) analysis at working acceleration voltage 200 kV. The crystal structure and type of the phases in a given area of the sample is determined (Table 2) by Selected Area Electron Diffraction (SAED). The presence of orthorhombic BSCCO phases 2223 and 2212 has been confirmed.

TEM image (Fig. 2), high resolution image (HR TEM) (Fig. 3.) and SAED analysis (Tables 2 and 3) of the BSCCO sample also confirm the presence of the two superconducting orthorhombic BSCCO phases - 2223 and 2212.

### Reduced graphene oxide (RGO)

The XRD pattern of reduced graphene oxide is shown in Fig. 4. The peaks in the XRD pattern prove that a monophasic product was successfully synthesized [30]. There are two main peaks in the X-ray diffractogram

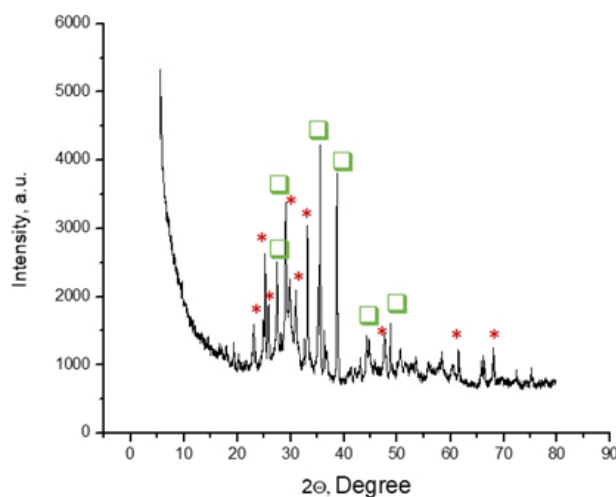


Fig. 1. XRD pattern of BSCCO.

Table 3. Phases determined by SAED analysis of BSCCO.

d [Å]	hkl	Phase
3.0715	00 10	$\text{Bi}_2\text{Sr}_2\text{CaCu}_2\text{O}_8$
2.5453	119	$\text{Bi}_2\text{Sr}_2\text{CaCu}_2\text{O}_8$
2.4096	211	$\text{Bi}_2\text{Sr}_2\text{CaCu}_2\text{O}_8$
2.3887	026	$\text{Bi}_2\text{Sr}_2\text{CaCu}_2\text{O}_8$
1.9725	219	$\text{Bi}_2\text{Sr}_2\text{CaCu}_2\text{O}_8$
1.7733	033	$\text{Bi}_2\text{Sr}_2\text{CaCu}_2\text{O}_8$
2.8150	119	$\text{Bi}_2\text{Sr}_2\text{Ca}_2\text{Cu}_3\text{O}_x$
2.6410	00 14	$\text{Bi}_2\text{Sr}_2\text{Ca}_2\text{Cu}_3\text{O}_x$
2.4560	00 15	$\text{Bi}_2\text{Sr}_2\text{Ca}_2\text{Cu}_3\text{O}_x$

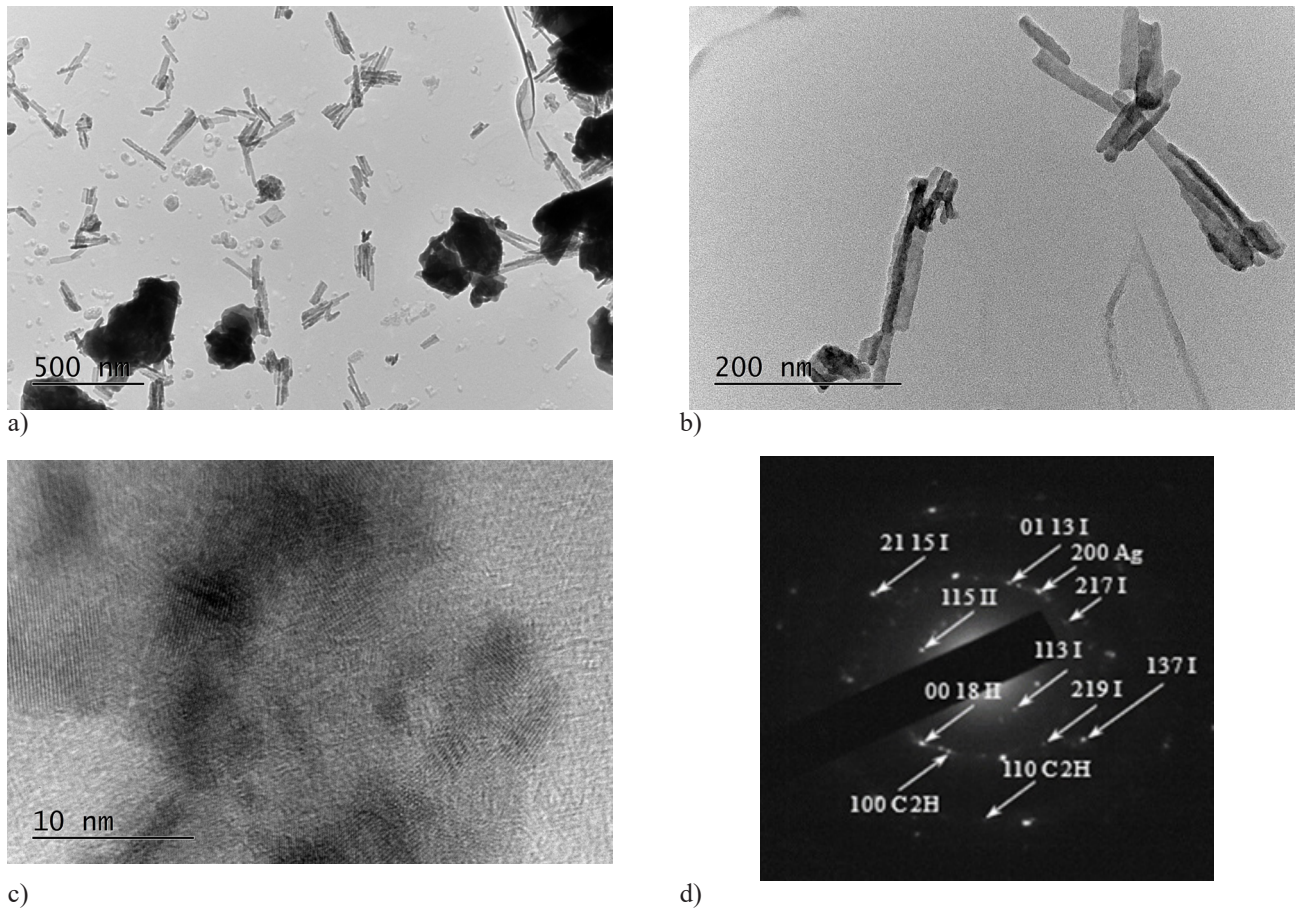


Fig. 2. TEM images a) at 10,000 x magnification, b) at 40,000 x magnification, c) HRTEM image at 600,000 x magnification and d) SAED (Selected Area Electron Diffraction) of BSCCO phases.

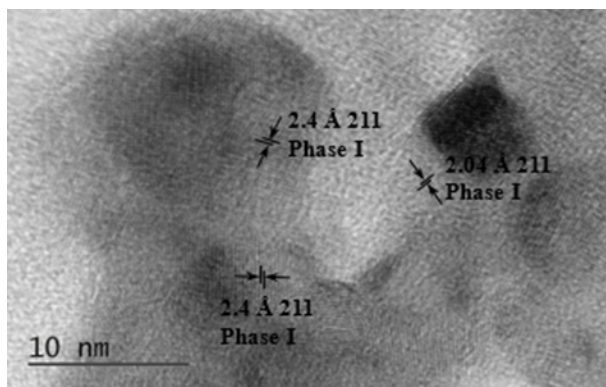


Fig. 3. High-resolution TEM image (HR TEM) (at 600,000 x magnification) of pure BSCCO ( $d = 2.4096 \text{ \AA } 211$ ,  $d = 2.0448 \text{ \AA } 128$  Phase I  $\text{Bi}_2\text{Sr}_2\text{CaCu}_2\text{O}_8$  COD #96-100-0286).

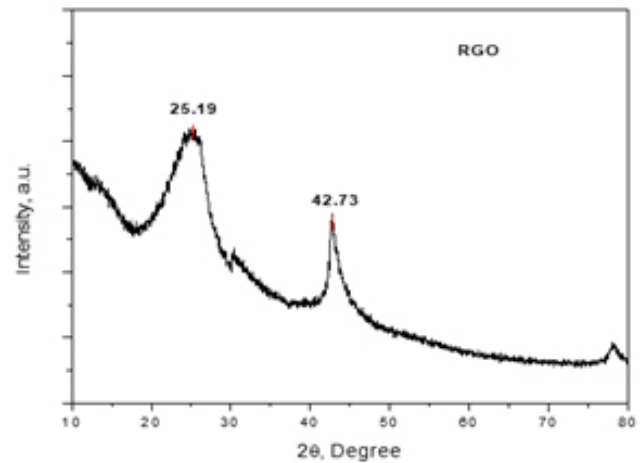
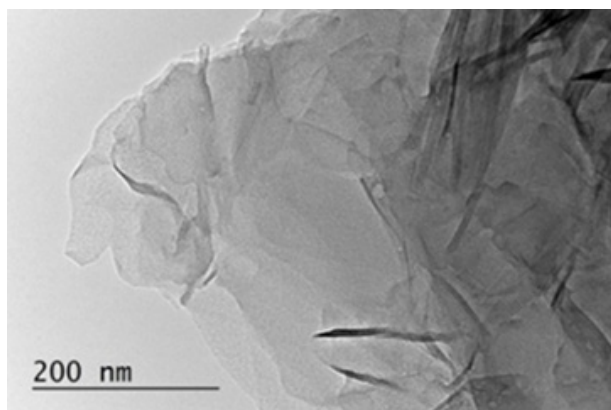


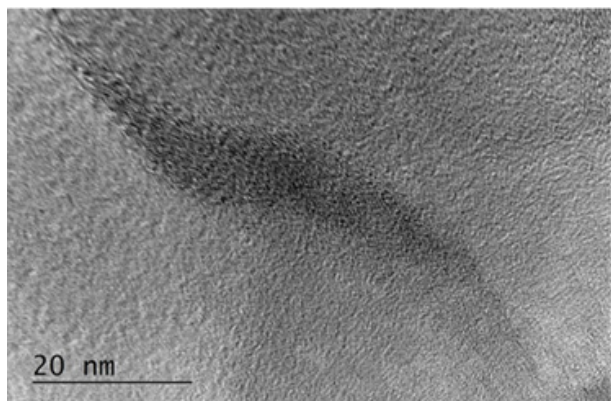
Fig. 4. XRD pattern of the obtained RGO.

of RGO: the first one at  $2\theta$  degree - 25.19 confirms the presence of reduced graphene oxide, and the second peak located at about  $2\theta$  degree - 42.70 is related to the (100) plane of the hexagonal carbon structure in the carbon layer [31, 32].

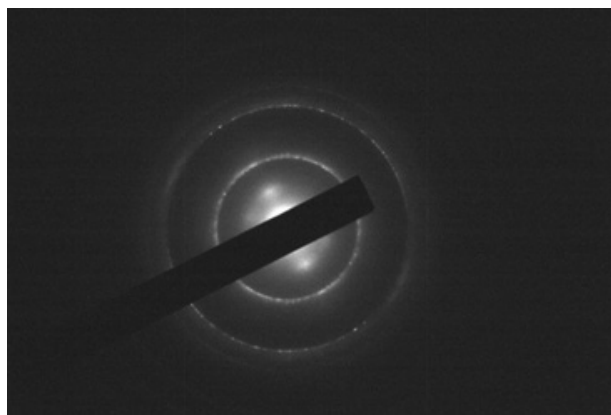
As reduced graphene oxide (RGO) contains one atom thick layers, TEM analysis is an appropriate



a)



b)



c)

Fig. 5. a) TEM image at 40,000 x magnification, b) High-resolution TEM image (HR TEM) at 600,000 x magnification and c) SAED (Selected Area Electron Diffraction) of RGO.

method for investigation of the graphene materials' structure. After the successful reduction, significant exfoliation of the graphene oxide layers was observed in the TEM images (Fig. 5). Smooth and singular graphene layers are obtained using our modified Hammer's method.

### Silver Nanoparticles (AgNPs)

The resulting powder of Ag nanoparticles was characterized using X-ray diffraction (Fig. 6). A comparison of the peak positions with the Crystallography Open Database shows that it corresponds to XRD card of Ag [JSPDS 00-901-1607 Silver].

Transmission electron microscopy is usually used to characterize materials with nano and atomic dimensions, so the method is suitable for the investigation of the obtained silver nanoparticle's structure. TEM image (Fig. 7), high resolution image (HR TEM) (Fig. 8.) and SAED analysis (Table 4) of the pure AgNPs sample confirm the presence of silver nanoparticles (Ag-cubic) with an approximate size of about 8 - 10 nm (Fig. 8(b)). In Fig. 8(a) silver aggregates are observed.

### BSCCO-RGO-AgNPs composites

All synthesized composites were characterized by using XRD analysis and Transmission electron microscopy. The XRD patterns of the composite materials BSCCO with the addition of 5 and 10 mass % AgNPs are presented in Figs. 9 and 10, respectively. As the amount of silver nanoparticles in the composite

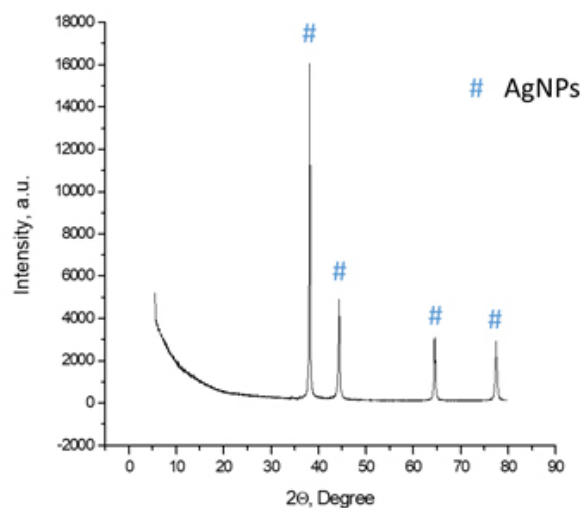


Fig. 6. XRD pattern of synthesized Ag NPs.

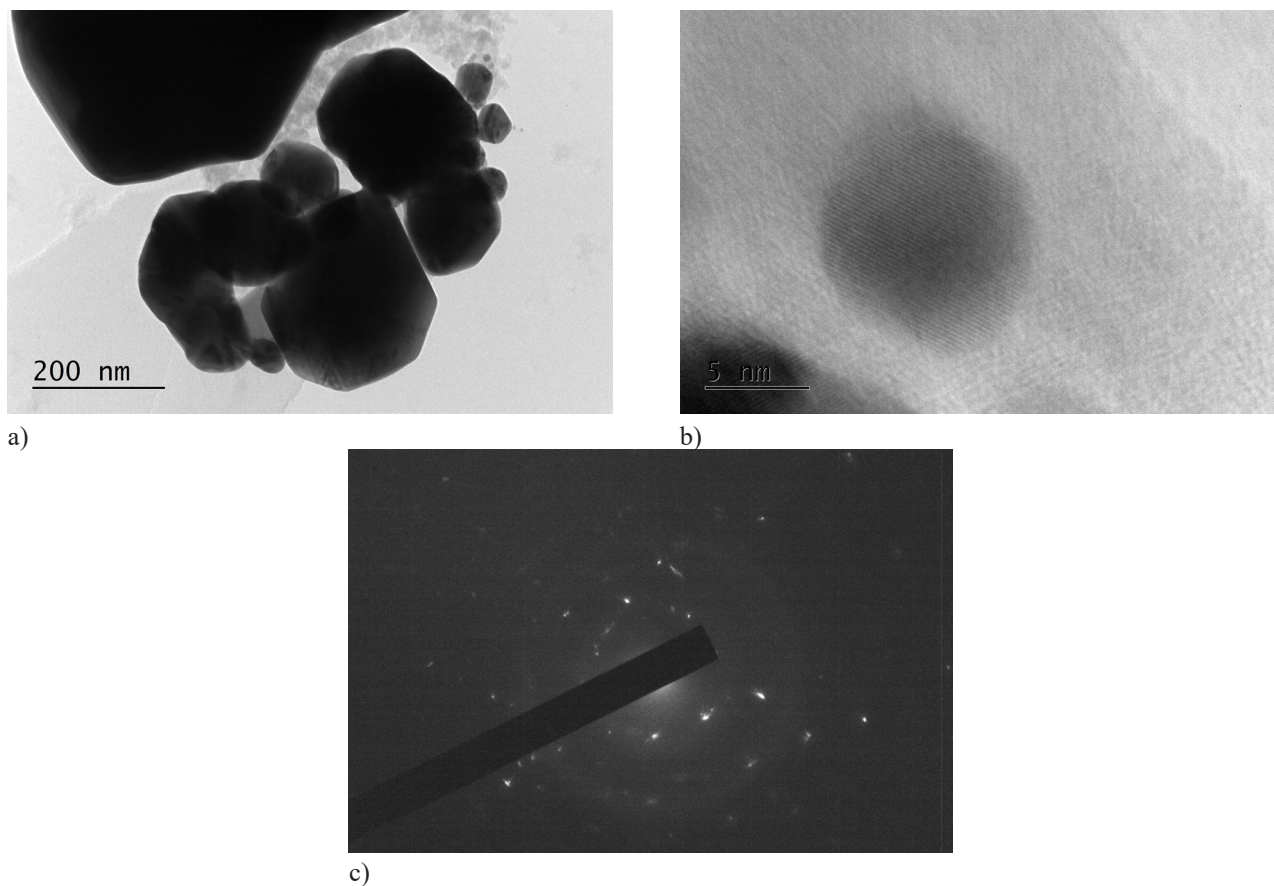


Fig. 7. a) TEM image at 30,000 x magnification, b) High-resolution TEM image (HR TEM) at 800,000 x magnification and c) SAED (Selected Area Electron Diffraction) of Ag NPs.

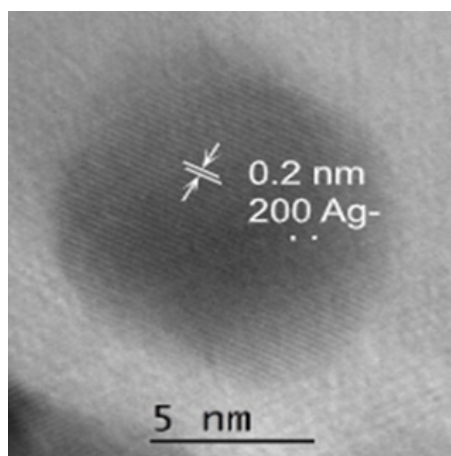


Fig. 8. High-resolution TEM image (HR TEM) (at 800,000x magnification) of Ag NPs ( $d = 2.0431 \text{ \AA}$  200 Ag-cubic COD #96-900-8460).

Table 4. Phase determined by SAED analysis in Ag NPs samples.

Phase	COD	Lattice parameters, [ $\text{\AA}$ ]	S.G.
Ag-cubic	#96-900-8464	$A = 4.07825$	Fm-3m

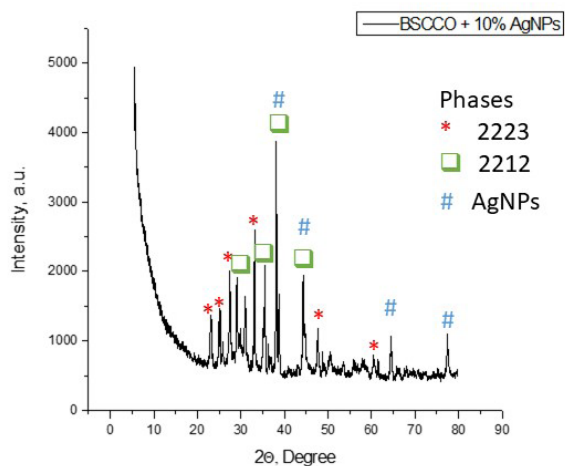


Fig. 9. XRD pattern of the composite material BSCCO + 5 mass % AgNPs.

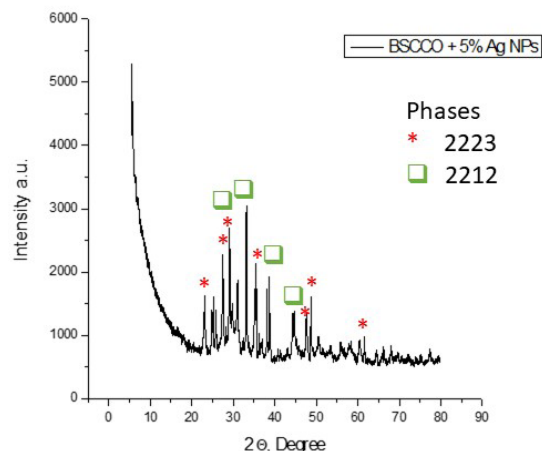


Fig. 10. XRD pattern of the composite material BSCCO + 10 mass % AgNPs.

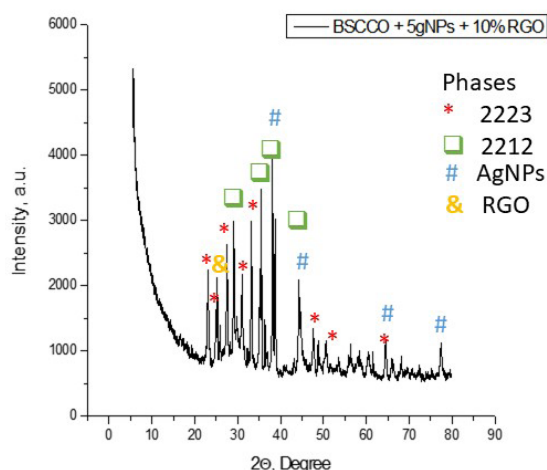


Fig. 11. XRD pattern of the composite material BSCCO + 5 mass % AgNPs + 10 mass % RGO.

(BSCCO + 5 mass % Ag NPs) is small, the intensities of silver peaks are not distinct in the XRD pattern in Fig. 9.

The silver peak at 38 degrees is clearly visible on the XRD pattern of the BSCCO + 10 mass % AgNPs composite in Fig. 10.

The XRD pattern of the BSCCO + 5 mass % AgNPs + 10 mass % RGO composite material is shown in Fig. 11. A characteristic peak of RGO with an intensity at 24 degrees is observed here in contrast to the XRD of the composites without the participation of RGO.

TEM image of the composite BSCCO + 5 mass % AgNPs + 10 mass % RGO confirms the presence of the two superconducting orthorhombic BSCCO phases - 2223 and 2212; silver nanoparticles (Ag-cubic) and RGO.

TEM image at 40,000 x magnification; High-resolution TEM images (HR TEM) at 600,000 x magnification and SAED (Selected Area Electron Diffraction) of the composite material BSCCO + 5 mass % AgNPs + 10 mass % RGO are presented in Fig. 12. It can be seen that the silver nanoparticles vary widely in size, which is probably due to their aggregation in different regions of the sample.

The distance  $d = 2.8815 \text{ \AA}$  117 in the presented high-resolution image in Fig. 13 of the composite material BSCCO + 5 mass % AgNPs + 10 mass % RGO corresponds to the phase  $\text{Bi}_2\text{Sr}_2\text{CaCu}_2\text{O}_8$ , (COD #96-100-0286). The crystal lattice parameters of the determined orthorhombic phase  $\text{Bi}_2\text{Sr}_2\text{CaCu}_2\text{O}_8$  are presented in Table 5.

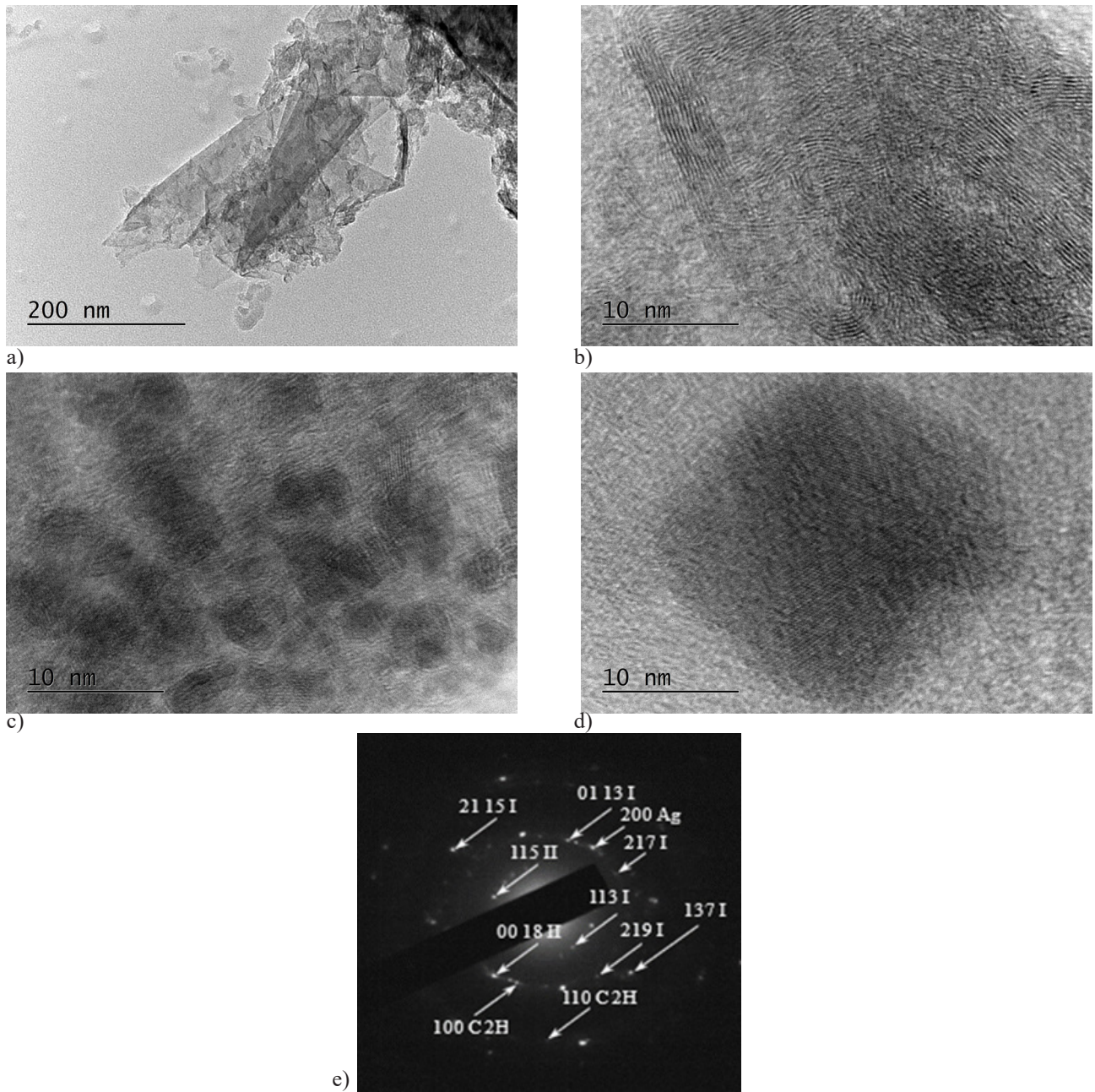


Fig. 12. a) TEM image at 40,000 x magnification; b) High-resolution TEM images (HR TEM); c) and d) at 600 000 x magnification; e) SAED (Selected Area Electron Diffraction) of the composite material BSCCO + 5 mass % AgNPs +10 mass % RGO.

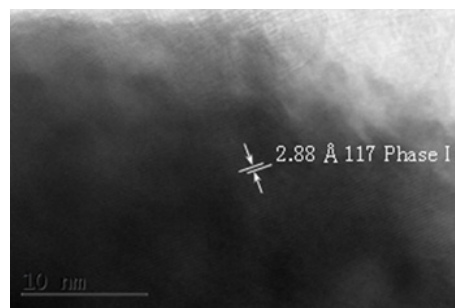


Fig. 13. High-resolution image (HR TEM) (at 600,000 x magnification) of the composite material BSCCO + 5 mass % AgNPs +10 mass % RGO ( $d = 2.8815 \text{ \AA}$  117, Phase  $\text{Bi}_2\text{Sr}_2\text{CaCu}_2\text{O}_8$ , COD #96-100-0286).

Table 5. Phases determined by SAED analysis of the composite BSCCO + 5 mass % AgNPs +10 mass % RGO.

	Phase	COD/PDF	Lattice parameters, [Å]	S.G.
I	Bi <sub>2</sub> Sr <sub>2</sub> CaCu <sub>2</sub> O <sub>8</sub> Orthorhombic	#96-100-0286	a = 5.4054 b = 5.4016 c = 30.7152	Amaa
II	Bi <sub>2</sub> Sr <sub>2</sub> Ca <sub>2</sub> Cu <sub>3</sub> O <sub>x</sub> Orthorhombic	45-1223	a = 5.42 b = 5.44 c = 36.76	
	Ag Cubic	#96-900-8460	a = 4.07825	Fm-3m
	Graphite 2H Hexagonal	#96-101-1061	a = b = 2.47 c = 6.79	P63mc

Table 6. Phases determined by SAED analysis.

d [Å]	hkl	Phase
3.5797	113	Bi <sub>2</sub> Sr <sub>2</sub> CaCu <sub>2</sub> O <sub>8</sub>
2.1647	01 13	Bi <sub>2</sub> Sr <sub>2</sub> CaCu <sub>2</sub> O <sub>8</sub>
2.1171	217	Bi <sub>2</sub> Sr <sub>2</sub> CaCu <sub>2</sub> O <sub>8</sub>
1.9725	219	Bi <sub>2</sub> Sr <sub>2</sub> CaCu <sub>2</sub> O <sub>8</sub>
1.5919	137	Bi <sub>2</sub> Sr <sub>2</sub> CaCu <sub>2</sub> O <sub>8</sub>
1.5624	21 15	Bi <sub>2</sub> Sr <sub>2</sub> CaCu <sub>2</sub> O <sub>8</sub>
3.4500	115	Bi <sub>2</sub> Sr <sub>2</sub> Ca <sub>2</sub> Cu <sub>3</sub> O <sub>x</sub>
2.0310	00 18	Bi <sub>2</sub> Sr <sub>2</sub> Ca <sub>2</sub> Cu <sub>3</sub> O <sub>x</sub>
2.0427	200	Ag
2.1391	100	C 2H
1.2350	110	C 2H

All the interplanar distances that correspond to the two superconducting phases (2212 and 2223), silver and graphene structures in the studied composite are presented in Table 6. The results of the TEM analysis confirm the data of the XRD patterns. The presence of the three components of the composite - superconducting phases, silver nanoparticles and graphene structures in the composite material BSCCO + 5 mass % AgNPs + 10 mass % RGO is proven.

## CONCLUSIONS

In the present study, composites with the participation of two superconducting phases Bi<sub>2</sub>Sr<sub>2</sub>CaCu<sub>2</sub>O<sub>8</sub> (2212) and Bi<sub>2</sub>Sr<sub>2</sub>Ca<sub>2</sub>Cu<sub>3</sub>O<sub>x</sub> (2223), silver nanoparticles and RGO were obtained. All the starting components and the obtained composites were structurally characterized by XRD, TEM, HRTEM and SAED (Selected Area Electron Diffraction) analysis. The preparation of the composite

materials and the presence of all the starting phases in them have been proven. The Ag nanoparticles size was determined in the range of 5 - 20 nm. From the TEM images, significant exfoliation of the graphene oxide was observed after the successful reduction. It can be seen that smooth and single graphene layers were obtained. TEM images of the composite BSCCO + 5 mass % AgNPs +10 mass % RGO confirmed the presence of the two superconducting orthorhombic phases BSCCO - 2223 and 2212; silver nanoparticles (Ag-cubic) with an approximate size of about 10 nm and the characteristic structure of RGO sheets.

The production of superconducting composites with the participation of Ag NPs and graphene structures aims improving the heat-conducting properties of superconducting ceramics by introducing of graphene and silver. As graphene and graphene materials have high thermal conductivity, this could enhance the thermal conductivity of superconducting composites. Until now, no such studies are known in the literature, and we want to make a start. In the future, the thermal conductivity of different compositions of superconducting composites with the participation of graphene layers in them will be investigated and it will be determined exactly how graphene structures and different metal nanoparticles can affect the thermal properties and superconducting parameters of superconducting nanocomposite materials.

## Acknowledgements

*This work was supported by Bulgarian National Scientific Fund, Grand KP-06-H27/17/17.12.2018.*

## REFERENCES

1. H. Maeda, Y. Tanaka, M. Fukutumi, T. Asano, A New High T<sub>c</sub> Oxide Superconductor without a Rare Earth

- Element, *Jpn. J. Appl. Phys.*, 27, 2, 1988, 209-210.
2. S. Cauffman, M. Blank, P. Cahalan, K. Felch, R.W. McGhee, M. Coffey, Operation of a 95 GHz 100 kW gyrotron in a high-T-c (BSCCO) magnet, IEEE, City, 2006.
  3. M. Kang, Y. Kim, H. Lee, G. Cha, K. Ryu, Magnetic field and critical current of a BSCCO HTS magnet at various aspect ratios, *IEEE Trans. Appl. Supercond.*, 21, 3, 2011, 2271.
  4. R.W. McGhee, E.E. Burkhardt, A. Berryhill, D.M. Coffey, Design and test results of a BSCCO-2223 magnet for gyrotron application, *IEEE Trans. Appl. Supercond.*, 15, 2, 2005, 1189.
  5. A.P. Malozemoff, D.T. Verebelyi, S. Fleshler, D. Aized, D. Yu, HTS wire: Status and prospects, *Physica C: Superconductivity and its Applications*, 386, 2003, 424-430.
  6. J.R. Hull, Applications of high-temperature superconductors in power technology, *Rep. Prog. Phys.*, 66, 11, 2003, 1865.
  7. W.V. Hassenzahl, Superconductivity, an enabling technology for 21st century power systems, *IEEE Trans. Appl. Supercond.*, 11, 1 II, 2001, 1447-1453.
  8. H.-G. Lee, G.-W. Hong, J.-J. Kim, M.-Y. Song, Role of silver on phase formation and texture development in Ag/BSCCO composites, *Materials Letters*, 23, 1-3, 1995, 65-68.
  9. R. Fluekiger, T. Graf, M. Decroux, C. Groth, Y. Yamada, Critical currents in Ag sheathed tapes of the 2223-phase in (Bi, Pb)-Sr-Ca-Cu-O, *IEEE Trans. Mag.*, 27, 1991, 1258.
  10. J.P. Singh, J. Joo, N. Vasanthamohan, R.B. Poeppel, Role of Ag additions in the microstructural development, strain tolerance, and critical current density of Ag-sheathed BSCCO superconducting tapes, *J. Mater. Res.*, 8, 1993, 2458-2464.
  11. M. Muralidhar, K. Nanda, Y. Ramana, V. Babu, Elastic and plastic behavior of lead and silver doped Bi-Sr-Ca-Cu-O superconductors, *Mater. Sci. Eng.*, B, 13, 1992, 215.
  12. A. Sotelo, M. Mora, M.A. Madre, J.C. Diez, L.A. Angurel, G.F. de la Fuente, Ag distribution in thick Bi-2212 floating zone textured rods, *J. Eur. Ceram. Soc.*, 25, 2005, 2947.
  13. N. Boussouf, M.F. Mosbaha, T. Guerfi, F. Bouancha, S. Chamekha, A. Amira, The effects of Ag, Mg, and Pr doping on the superconductivity and structure of BSCCO, *Physics Procedia*, 2, 2009, 1153-1157.
  14. S.S. Oh, H.S. Ha, D.W. Ha, H.M. Jang, C. Park, Development of Bi-2223 HTS tape and its application to coil and current leads, *Cryogenics*, 42, 2002, 377.
  15. J.B. Torrance, Y. Tokura, S.J. LaPlaca, T.C. Huang, R.J. Savoy and A.I. Nazzari, New class of high  $T_c$  structures: Intergrowth of multiple copper oxide perovskite-like layers with double sheets of BiO, *Solid State Commun.*, 1988, 66 703.
  16. R. Mertens, *Graphene Handbook*, Edition 2021, <https://www.graphene-info.com/graphene-thermal>
  17. J.D. Renteria, D.L. Nika and A.A. Balandin, *Graphene Thermal Properties: Applications Management and Energy Storage*, *Appl. Sci.*, 4, 2014, 525-547.
  18. K.M.F. Shahi and A.A. Balandin, *Graphene-Multilayer Graphene Nanocomposites as Highly Efficient Thermal Interface Materials*, *Nano Lett.*, 12, 2012, 86.
  19. F. Yavari, H.R. Fard, K. Pashay, M.A. Rafiee, A. Zamiri, Z. Yu, R. Ozisik, T. Borca-Tasciuc and N. Koratkar, Enhanced Thermal Conductivity in a Nanostructured Phase Change Composite due to Low Concentration Graphene Additives, *J. Phys. Chem. C*, 115, 2011, 8753.
  20. J. Hu, W. Park, X. Ruan, Y.P. Chen, Thermal Conductivity Measurement of Graphene Composite, *Mater. Res. Soc. Symp. Proc.*, 2013, 1456.
  21. M. Colie, D. Mihaiescu, A. Surdu, R. Trusca, B. Vasile, D. Istrati, A. Ficai, C. Plapcianu, E. Andronescu, High temperature superconducting materials based on Graphene/YBCO nanocomposite, 6th International conference on Advanced Nano Materials, *Materials Today: Proceedings*, 3, 2016, 2628-2634.
  22. S. Dadras, S. Dehghani, M. Davoudiniya, S. Falahati, Improving superconducting properties of YBCO high temperature superconductor by Graphene Oxide doping, *Materials Chemistry and Physics*, 193, 2017, 496-500.
  23. B. Sahoo, K.L. Routray, D. Samal, Dhruvananda Behera, Effect of artificial pinning centers on YBCO high temperature superconductor through substitution of graphene nano-platelets, *Materials Chemistry and Physics*, 223, 2019, 784-788.
  24. S. Yang, J. Zhang, Deposition of YBCO nanoparticles on graphene nanosheets by using matrix-assisted pulsed laser evaporation, *Optics and Laser*

- Technology, 109, 2019, 465-469.
25. S.-J. Sun, H. Chou, Triplet superconducting p+ip pairs existing in a graphene sandwiched by superconductor and ferromagnet, *Physics Letters A*, 382, 2018, 3012-3017.
  26. S. Dadras, S. Falahati, S. Dehghani, Effects of graphene oxide doping on the structural and superconducting properties of  $\text{YBa}_2\text{Cu}_3\text{O}_{7-\delta}$ , 548, 2018, 65-67.
  27. J. Mateeva, A. Staneva, B. Martinov, B. Blagoev, T. Nurgaliev, Synthesis and characterization of YBCO and YBCO/Ag superconducting ceramic composites containing reduced graphene oxide, *J. Chem. Technol. Metall.*, 54, 4, 2019, 1215-1222.
  28. A. Staneva, J. Mateeva, B. Martinov, B. Blagoev, T. Nurgaliev, Effect of graphene oxide and reduced graphene oxide on electrical properties of YBCO and YBCO/Ag composites, *J. Chem. Technol. Metall.*, 55, 2, 2020, 359-366.
  29. U. Balachandran, D. Shi, D.I. Dos Santos, S.W. Graham, M.A. Patel, B. Tani, K. Vandervoort, H. Claus and R.B. Poeppel, 120 K superconductivity in the (Bi, Pb)-Sr-Ca-Cu-O system, *Physica C*, 156, 1988, 649.
  30. V. Gunasekaran, K. Krishnamoorthy, R. Mohan, S-J. Kim, An investigation of the electrical transport properties of graphene-oxide thin films, *Mater. Chem. Phys.*, 132, 2012, 29-33.
  31. M. Khenfouch, U. Buttner, M. Baitoul and M. Maaza, Synthesis and Characterization of Mass Produced High Quality Few Layered Graphene Sheets via a Chemical Method, *Graphene*, 3, 2014, 7-13
  32. Y. Zhan, F. Meng, Y. Lei, R. Zhao, J. Zhong, X. Liu, One-pot solvothermal synthesis of sandwich-like graphene nanosheets/ $\text{Fe}_3\text{O}_4$  hybrid material and its microwave electromagnetic properties, *Materials Letters*, 65, 2011, 1737-1740.